



# Forestlines in Italian mountains are shifting upward: detection and monitoring using satellite time-series

Lorena Baglioni<sup>1</sup>, Donato Morresi<sup>2</sup>, Matteo Garbarino<sup>3</sup>, Carlo Urbinati<sup>1</sup>, Emanuele Lingua<sup>4</sup>, Raffaella Marzano<sup>3</sup> and Alessandro Vitali<sup>1</sup>

5 <sup>1</sup>Department of Agricultural, Food and Environmental Sciences, Marche Polytechnic University, Ancona, Italy

<sup>2</sup>Department of Forest Resource Management, Swedish University of Agricultural Sciences, Umeå, Sweden

<sup>3</sup>Department of Agricultural, Forest and Food Sciences, University of Torino, Torino, Italy

<sup>4</sup>Department of Land, Environment, Agriculture and Forestry, University of Padova, Padova, Italy

10 *Correspondence to:* Lorena Baglioni (*lorena.baglioni@pm.univpm.it*)

**Abstract.** The growing interest on the ecological effects of global warming and land use changes on vegetation, along with development of remote sensing techniques, fostered applied research on the successional dynamics at the upper limits of forests. The aims of this study were: i) to develop an automated methodology for mapping the current position of the uppermost italian forestlines; ii) to identify hotspots of change by the analysis of long-term greenness and wetness spectral dynamics. We carried on a Landsat-based trend analysis in buffer zones along the forestlines, testing differences between sparse and dense canopy cover classes and at different elevations and distances to the forestline. We used regional scale datasets and avoided to fix a minimum elevation threshold, in order to make the method replicable at different mountain ranges. For the spectral dynamics analyses, we used Landsat time-series of common vegetation indices for the period 1984–2023 and tested the significance of their long-term spectral trends with the Contextual Mann-Kendall test for monotonicity. We assessed that the highest forestlines are at the western sector in the Alps, and at the central one in the Apennines. We observed a common increase of the forest cover mainly close to the forestline and at lower elevations. Comparing greenness and wetness indices trends with the current canopy cover, the highest values were respectively in the sparse tree cover class, and in the dense one, particularly in the Alps.

25 **Keywords:** Landsat, remote sensing, Contextual Mann Kendall, treeline, spectral vegetation index.



## 1. Introduction

A treeline is the contiguous ecotone along an altitudinal or latitudinal gradient (Körner, 2008; Berdanier, 2010; Harsch et al., 2011).

Nowadays, treeline studies concern spatio-temporal dynamics to climate and/or land use changes (Malanson et al., 2011).

30 Current treeline elevation and its spatial patterns derive from air temperature increase and past human activities that have modified treeline physiognomy and dynamics over time (Holtmeier et al., 2005; Harsch et al., 2011). Most European mountain landscapes have been shaped by humans since prehistoric times through fire, deforestation and intensive grazing (Malanson et al., 2011; Vitali et al., 2018; Garbarino et al., 2020). In the Mediterranean region, the treeline elevation is therefore much lower than its potential climatic position (Körner 2012; Piper et al., 2016). Moreover, human activities have locally altered, 35 directly or indirectly, species composition (Obojes et al., 2024) and induced new disturbances. For instance, in western Alps favouring *Larix decidua* Mill to *Pinus cembra* L. and promoting an invasive resprouter like *Alnus viridis* (Chaix) DC. (Dziomber et al., 2024, Motta et al., 2006). In the Apennines planting *Pinus nigra* at high altitude facilitated its upward encroachment in treeline ecotones (Vitali et al., 2017). It is therefore reasonable to associate the upward advancement not only to global warming (Hansson et al., 2023) but also to successional dynamics (Ameztegui et al., 2016; Vitali et al., 2017) and to 40 geomorphic processes (Leonelli et al., 2009). The ongoing development of remote sensing techniques and geographic information systems provided new opportunities in treeline studies (Holtmeier et al., 2020) such as detecting and monitoring the dynamic patterns of treeline shape and density (Fissore et al., 2015). Defining clear and easily replicable methods based on the application of modern technologies accessing to available datasets is fundamental for an accurate and large-scale treelines monitoring. At the local scale, aerial photography is commonly used (Ameztegui et al., 2016; Hansson et al., 2020; 45 Nguyen et al., 2024) despite its limits due to image quality and availability (Morley et al., 2018). At larger scales, He et al. (2023) detected closed-loop mountain treelines integrating high resolution tree cover maps and digital elevation models, whereas Wei et al. (2020) in the Western United States proposed an “alpine treeline ecotone detection index” (ATEI) based on the analysis of altitudinal and normalized difference vegetation index (NDVI) gradients. At the regional scale, supervised and unsupervised classification of multispectral images are widely used (Fissore et al., 2015, Chhetri and Thai, 2019), as well 50 as detection techniques based on land cover maps combined with digital elevation models (e.g. Pecher et al., 2011).

Besides mapping, ongoing treelines research includes its spatio-temporal dynamics. Despite the coarser spatial resolution and the limitation of cloud cover, satellite optical imagery offers a finer time resolution by integrating data from several platforms and free processed time-series. It also provides spectral information for synchronic analysis of vegetation changes (Gómez et al., 2016). After the open access to its database in 2008, the use of Landsat time-series has increased in recent decades (Zhu, 55 2017). Due to their spatial resolution (30 m) and temporal data availability, Landsat images have been largely used for vegetation dynamics monitoring, such as post-disturbance forest recovery (Morresi et al., 2019), greening or browning in different ecosystems (Bayle et al., 2024; Kumar et al., 2022; Rumpf et al., 2022) and to study alpine treelines applying greening proxies like vegetation indices (Fissore et al., 2015; Tian et al., 2022). The NDVI is widely used in treeline dynamics, being



more sensitive in detecting biomass changes in open rather than in closed canopies (Choler et al., 2021; Wei et al., 2020; Arekhi et al., 2018; Bharti et al., 2012; Zou et al., 2022; Bayle et al., 2025). In the European Alps, Carlson et al. (2017) and Choler et al. (2021) used the annual maximum NDVI max values (NDVI-max) to analyse the greening trends from Landsat and MODIS time-series. They assessed a significantly increasing spectral trend over the last two decades, mainly at north-facing slopes and in sparsely vegetated areas. Nevertheless, Bayle et al. (2024) remarked that the higher number of Landsat observations throughout the growing seasons can affect the NDVI-max trend analysis, causing false outcomes. It is true that annual NDVI-max increase with the number of available observations, and therefore their frequency must be taken into account. In the southwestern part of the European Alps, Bayle et al. (2025) studied greening trends using the annual max of kernel normalized difference vegetation index (kNDVI) (Camps-Valls et al., 2021), a nonlinear version of the NDVI, overcoming the overestimation of greening by the Harmonic Analysis of Time Series (HANTS), as reported by Choler et al. (2024). Bolton et al. (2018), instead, used the Enhanced Vegetation Index (EVI) for a Landsat based greening trend analysis of alpine treelines in the Canadian boreal zone. The EVI corrects the aerosol influence and canopy background noise and it is less affected by saturation than NDVI, being more sensitive to the NIR band (Huete et al. 2012). For this reason, it can detect the spectral behaviour of lower layers of vegetation while NDVI responds mainly to the RED band, which is involved in photosynthetic activity of the upper canopy layer. A single index can be combined with other vegetation indices to reduce the uncertainty on change detection analysis (Zhou et al., 2023; Schultz et al., 2016). EVI and NDVI can be considered greenness indices since they are linked to the photosynthetic activity of vegetation by using NIR and RED bands, while wetness indices introduce short-wave infrared (SWIR) bands that are especially sensitive to water content of vegetation (Huete, 2012). Examples of wetness indices are the normalized difference moisture index (NDMI) and the normalized burn ratio index (NBR). This kind of indices are sensitive to shadowing, forest structure, leaf internal structure, vegetation moisture and density (Schroeder et al., 2011). In Landsat-based forestry applications, indices derived from the Tasseled Cap Transformation (TCT) (Kauth and Thomas, 1976; Crist and Cicone, 1984) are also commonly used, since they are less affected by soil reflectance (Cohen and Goward, 2004). The Tasseled Cap Wetness index (TCW) considers the visible bands and both the SWIR1 and the SWIR2, and it is suitable to predict forest structural attributes, being slightly influenced by topographic variations, especially in closed conifer stands (Cohen et al., 1995). Another TCT index is the Tasseled Cap Angle (TCA) (Powell et al., 2010), combining the greenness and brightness information as defined in Crist and Cicone (1984) to assess the ratio between vegetated and non vegetated areas (Gómez et al., 2011). In our study we considered “forestline” the line separating the closed forest from the shrubland and grassland above, and “treeline” or “forestline ecotone” the surrounding area, the spatial pattern of which was not investigated due to the scale of analysis adopted. Forestlines ecotones are dynamic ecosystems and their monitoring on a regional scale can be carried on through the analysis of their spectral behaviour over time adopting different indices and tools. In this context, our study analyzed forestlines dynamics in the main Italian mountain ranges, the Alps and the Apennines. Our aims were

- 1) To define and monitor the position of the uppermost forestlines through an automated methodology;



- 2) To identify hotspots of change through satellite data, verifying whether and where forest recolonization dynamics are occurring.

95 In particular, we analysed the long-term greenness and wetness spectral changes of the uppermost forests and the contiguous forestline ecotones using Landsat-based trend analysis of time-series for the period 1984-2023, and we tested if greenness and wetness indices trends differed with elevation, forestline distance and canopy cover densities.

We hypothesised that greenness indices are more fitted for forest recolonization of open areas, while wetness ones for detecting gap-filling processes intercepting the spectral signal of lower leaf strata.

100

## 2. Materials and methods

### 2.1. Study area

The Alps and the Apennines are the two mountain ranges of the Italian peninsula. They extend respectively for 1300 and 1350 km: the Alps from West-to-East across northern Italy; the Apennines from NW to SE.. They also differ in climate, elevation range, and vegetation characteristics. In the Alps, annual precipitation range between 400 and 3000 mm, with rare summer dry periods and cold winters (Isotta et al., 2014). Conifer forests prevail in the subalpine zone, where the main species are Norway spruce (*Picea abies* (L.) H.Karst.), European larch (*Larix decidua* Mill.) and/ or Swiss stone pine (*Pinus cembra* L.) (Fauquette et al., 2018). In the Apennines, the total annual precipitation range between 600 and 4500 mm (Vacchiano et al., 2017), with short and pronounced summer dry periods (Blasi et al., 2014). Mixed broadleaf forests dominate at lower elevation, while Common beech (*Fagus sylvatica* L.), locally mixed with silver fir (*Abies alba* Mill.), is the main species in the montane zone, except for rare locations in the central and southern parts of the Apennines, where also mountain pine (*Pinus mugo* Turra), European black pine (*Pinus nigra* J.F. Arnold), and Bosnian pine (*Pinus heldreichii* H.Christ) occur naturally. We selected the highest peak for each mountain group of the Alps and the Apennines, as defined by the Global Mountain Biodiversity Assessment (GMBA) inventory (Snethlage et al., 2022a, 2022b). We located the exact position of the peaks using the nationwide Tinitaly Digital Elevation Model (DEM) v 1.1 (Tarquini et al., 2023). We then filtered the mountain groups and retained only the ones with highest peaks located on bare soil or in snow/ice covered areas, according to the Dynamic World land cover map (Brown et al., 2022). In this way we excluded also the mountain groups completely covered by forest or affected by severe human impacts, such urban or built-up areas. In addition, for excluding the mountain peaks lacking the alpine belt thermoclimatic characteristics, we used the orotemperate, cryorotemperate and gelid thermotypes, derived from the Bioclimates of Italy dataset (Pesaresi et al., 2017) based on the Worldwide Bioclimatic Classification System (WBCS) by Rivas-Martínez (1993). Others GMBA mountain groups have been removed after the previous selection based on land cover

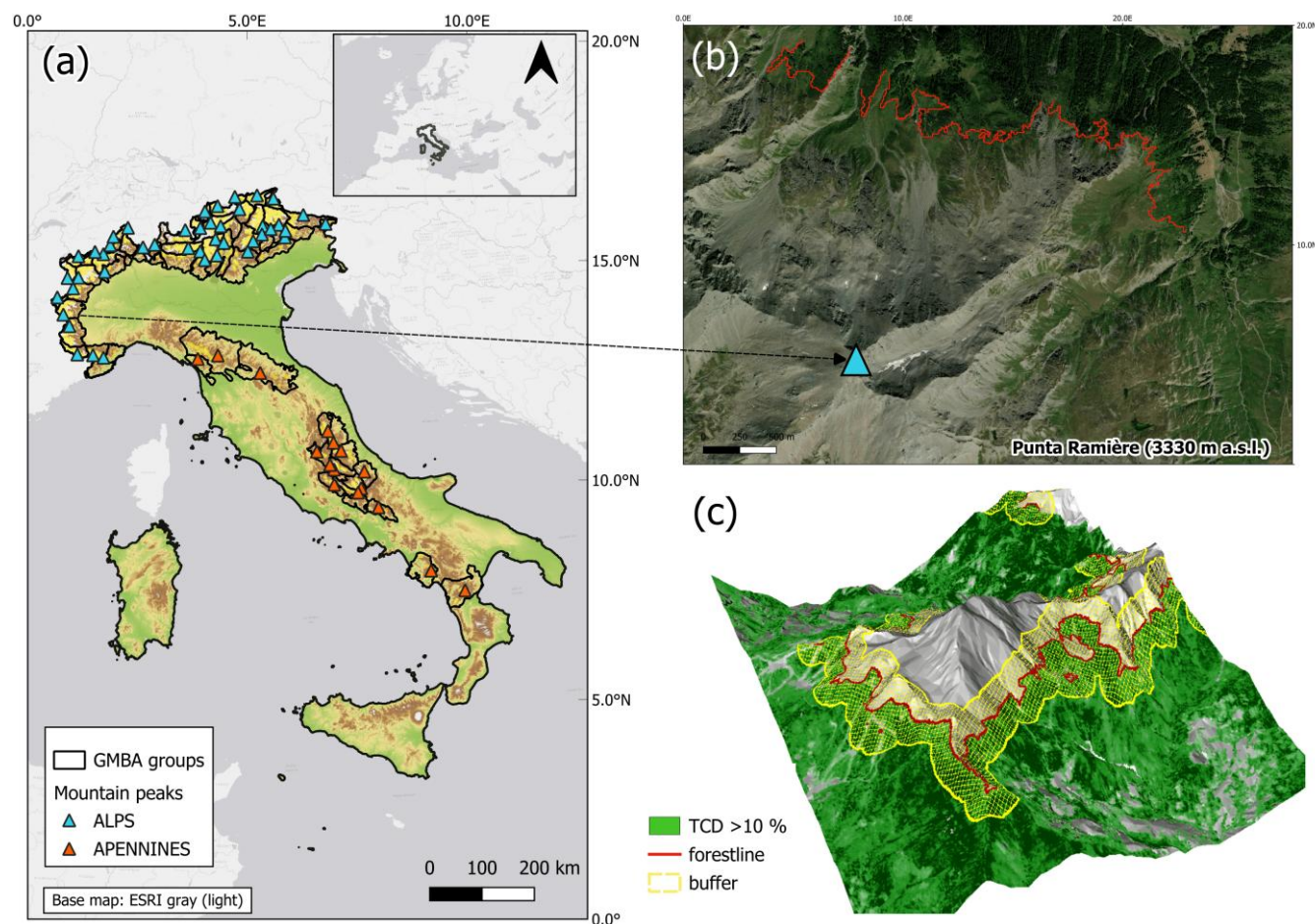


and bioclimatic parameters, because of the Italian administrative and GMBA's boundaries limited the altitudinal range and forest distribution of some groups on the border in the following analyses (Sect. 2.2).

## 125 2.2. Detection of forestlines

We used the Tree Cover Density 2018 (TCD) of the European Environment Agency (EEA) derived from Sentinel-2 multispectral data as a reference for forest cover. TCD has a 10 m spatial resolution and provides information about the percentage of crown coverage in each pixel. According to the FAO "forest" definition (FAO, 2000), we selected only pixels having a TCD higher than 10 % to obtain a mask of forested areas. For each mountain group, we obtained the vertical distance  
130 between each forest pixel and the DEM derived highest peak. We then selected the forest pixels with a vertical distance within the 1<sup>st</sup> percentile of all the distances and extracted the contours of the forestline by considering only the side of each selected forest pixel facing the mountain peak. We decided to not define a minimum altitudinal threshold to allow the method replicability on other mountain ranges of different elevations. Then, we joined polylines with linear gaps shorter than 30 m (corresponding to the Landsat spatial resolution). We considered only resulting polylines longer than 500 m to avoid highly  
135 fragmented forestlines and to focus on more spatially extended and continuous ecotones and we removed closed loops to exclude the edges of forest gaps below the forestline. We outlined an area of interest around the uppermost forestlines where directing the analysis. Indeed, we defined a buffer zone of 250 m radius (Fig. 1c) along the lines to assess the presence of significant spectral changes in a gradient from closed forest to grassland. We also sampled points at 10 m distance along the detected forestlines to assess the mean, median and maximum elevation of all the detected forestlines, grouped by mountain  
140 groups or mountain ranges. We processed the data in the R software environment (v. 4.3.2) using the "terra" (Hijmans, 2023), "callr" (Csárdi and Chang, 2024) and "future.apply" (Bengtsson, 2021) packages, and with QGIS software (v. 3.34.1).





145 **Figure 1 - (a) Selected peaks (triangles) along the Italian Alps (light blue) and Apennines (orange); (b) Detected forestlines (red**  
**polylines) on a ESRI satellite image (ArcGIS/World Imagery) of Punta Ramière (3330 m a.s.l.) in the Montgenèvre Alps GMBA**  
**group; (c) a 3D graphical model based on the Tinitaly DEM and the TCD forest mask (TCD >10 %) used for the forestlines detection**  
**and the buffer area definition (yellow area).**

### 150 2.3. Trend analysis of vegetation indices

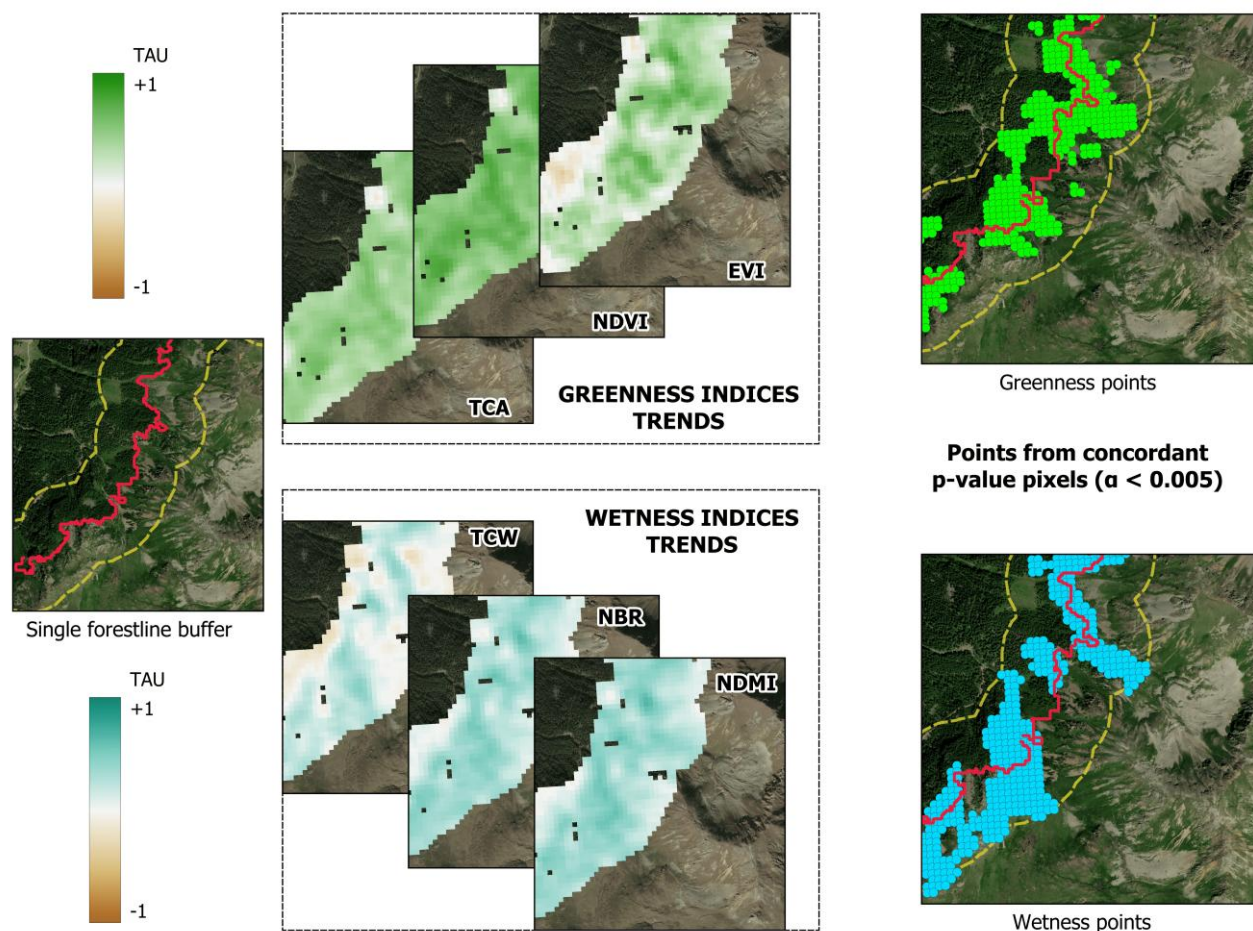
Landsat data provide medium resolution images (30 m pixel size) from 1984 to 2023, that are commonly used in treeline studies (Arekhi et al., 2018, Bharti et al., 2012, Morley et al., 2019, Garbarino et al., 2024) since they offer a good compromise between space and time resolution (Hansson et al., 2020) at regional scale. We collected multispectral images from June 1<sup>st</sup> to September 30<sup>th</sup> of each year to analyse the spectral behaviour of forest vegetation during the growing season and to reduce the effect of snow cover and alpine meadows drying up during the summer months.



In particular, we used Landsat Level-2 Collection 2 images acquired by the TM, ETM+, OLI and OLI-2 sensors. After masking pixels covered by snow, clouds, cloud shadows and water, we produced reflectance composites based on the medoid compositing approach (Flood 2013). We computed common vegetation indices from reflectance composites that we grouped into i) greenness indices: normalized difference vegetation index (NDVI) (Tucker, 1979), enhanced vegetation index (EVI) (Huete et al., 2002) and tasseled cap angle index (TCA) (Powell et al., 2010); and ii) wetness indices: normalized burn ratio (NBR) (García et al., 1991), normalized moisture index (NDMI) (Gao, 1996) and tasseled cap wetness index (TCW) (Crist, 1985). Finally, we masked the 40 year-long time-series using the buffer areas around each selected forestline (Sect. 2.2). We assessed the significance in the monotonicity of the spectral trends, i.e. strictly increasing or decreasing, derived from vegetation indices time-series by applying the non-parametric Contextual Mann Kendall (CMK) statistical test (Neeti et al., 2011). The CMK test is an estimator of the monotonicity of trends, based on the Mann-Kendall (MK) test, which takes into account the trends in the neighbouring pixels within a 3 x 3 kernel. In this way, the spatial autocorrelation is considered, thus improving the detection of spatial patterns characterised by homogeneous spectral trends. Specifically, we used the “ConMK” R package (available at <https://github.com/geoportishare/ConMK>). The TAU statistics produced by the MK test ranges between +1 and -1, with positive values indicating an increasing trend, while negative values are associated with decreasing trends. Before checking the occurrence of significant trends by computing the p-value ( $\alpha$ ) associated with the TAU statistics, we pre-processed time-series in two steps. First, we filled missing data at the pixel level through linear interpolation and considering also one-year gaps while discarding pixels with longer data gaps. Second, we removed the autocorrelation in the time-series by applying the pre-whitening procedure proposed by Wang and Swail (2001) and implemented in the “ConMK” R package.

#### 2.4. Assessment of the spectral trends

For each group of vegetation indices, i.e. greenness and wetness, we selected only those pixels that exhibited a highly significant trend ( $\alpha < 0.005$ ), as proposed in Choler et al. (2021) for all the indices (Fig. 2).



180 **Figure 2 - Example of the extraction of the highly significant ( $\alpha < 0.005$ ) greenness (top) and wetness (bottom) points trends in the buffer area (yellow dotted line) around a single forestline (full red polyline). Base map: ESRI Satellite (ArcGIS/World\_Imagery).**

We used the points corresponding to the resulting pixel centroids to extract the mean TAU value among the vegetation indices  
 185 and the elevation from the Tinitaly DEM. The original TCD excludes shrublands, dwarf pine or green alder in alpine areas (Copernicus Land Monitoring Service, 2021) but we resampled it to 30 m by average and assigned to each pixel centroid also the mean tree canopy cover.

Then, we excluded points with negative trends ( $\text{TAU} < 0$ ) and with  $\text{TCD} = 0$  that corresponded to areas without a tree canopy  
 190 dynamics different from forest recolonization. We assigned the elevation value of the nearest forestline point to the resulting wetness and greenness points using the “join attributes by nearest” tool in QGIS. In this way, we obtained the Euclidean distance of each trend point to the forestline and the difference in elevation, which we used to classify the points into above or below the forestline. Specifically, we identified the relative position to the forestline of each points by multiplying the





Euclidean distances by the sign of the difference in elevation. We carried out the analysis by considering the Alps and Apennines separately, due to their altitudinal, climatic and vegetation differences, as previously described (Sect. 2.1). For each mountain range, we obtained two sets of 40.000 randomly sampled points, broadly containing a equal number of greenness and wetness significant trends. We then grouped the sampled points into three tree canopy cover categories according to TCD: i) sparse canopy cover (TCD <10 %); ii) moderate-to-dense canopy cover (10 % < TCD < 80 %); iii) dense canopy cover (TCD > 80 %). We then assessed the relationship between TAU values and the canopy cover, the elevation and the distance to forestline, taking into account the mean values of each segment of forestline. We used a Wilcoxon test (Wilcoxon, 1945) to verify significant differences between the mean TAU among wetness and greenness indices averaging the mean TAU values of each canopy cover class in each forestline buffer. Finally, we built Generalized Additive Models (GAM) (Hastie and Tibshirani, 1990) using the cubic spline smoother of the “mgcv” R package (Wood, 2011) to test the presence of a significant non-linear relationship between the mean TAU values and i) the elevation and ii) the distance to forestline, without considering the TCD classes.

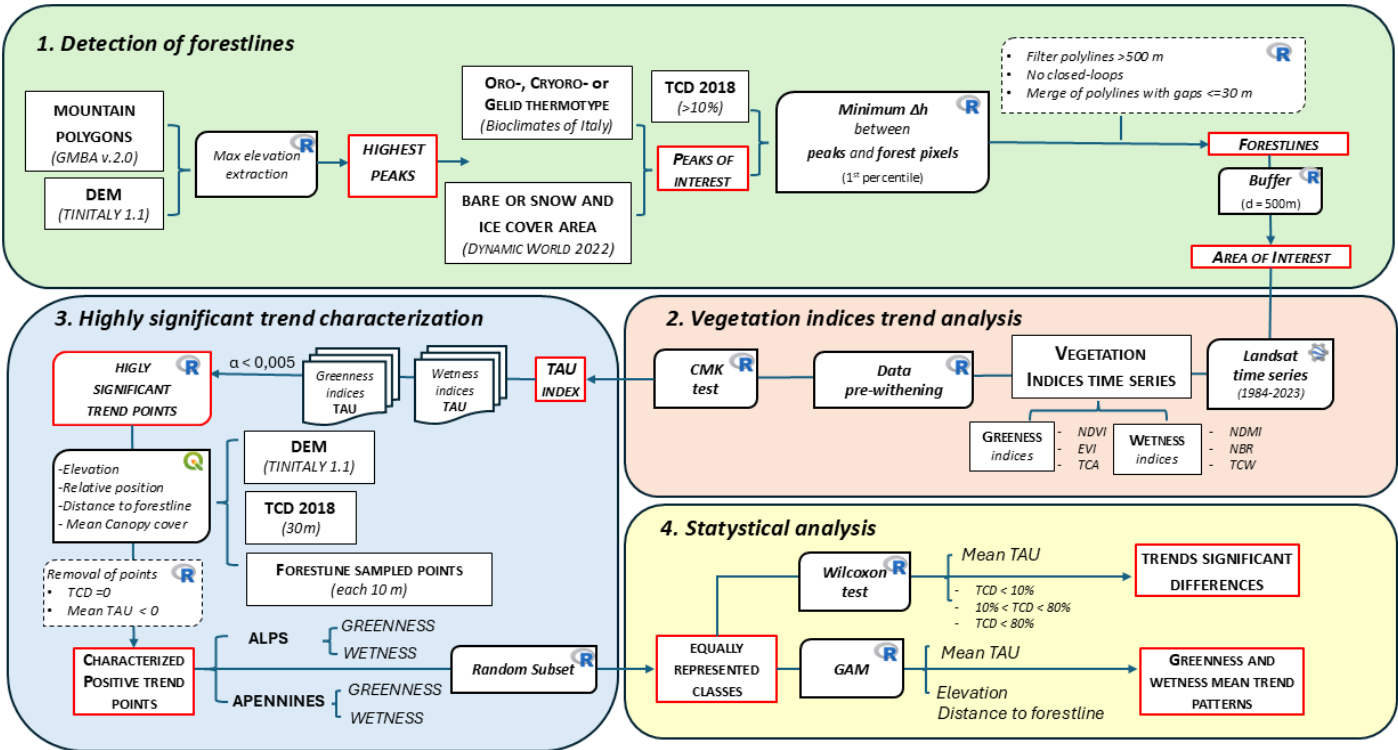


**Figure 3 – Flow chart of the analytical process: input data (black rectangles), outputs (red rectangles) and analyses (irregular rectangles). Abbreviations: DEM (digital elevation model), TCD (tree cover density), NDVI (normalized difference vegetation index), EVI (enhanced vegetation index), TCA (tasseled cap angle index), NDMI (normalized difference moisture index), NBR (normalized burn ratio), TCW (tasseled cap wetness index), CMK (contextual mann-kendall test), GAM (generalized additive model).**

### 3. Results

#### 3.1. Forestlines extraction

We identified and processed 60 mountain peaks, 44 in the Alps and 16 in the Apennines (Table A1-Appendix A). We obtained approximately 5760 km of forestlines with a mean elevation of  $2088 \pm 193$  m a.s.l. in the Alps and  $1758 \pm 161$  m a.s.l. in the Apennines, with a maximum elevation respectively of 2500 and 2383 m a.s.l. In the Alps, the lowest forestline elevations were in the prealpine groups due to the lack of a suitable altitudinal gradient, whereas the highest ones were mainly in the western sector (Fig. 4a). In the Apennines, the lowest and less extended forestlines, if compared to the forested area, were in the northern sector, while the highest ones were in Central Italy: the Majella (MJ), Sirente Velino (SVE) and Marsicani (MM) mountain groups (Fig. 4b). The total area of interest obtained was of approximately 1880 km<sup>2</sup>.

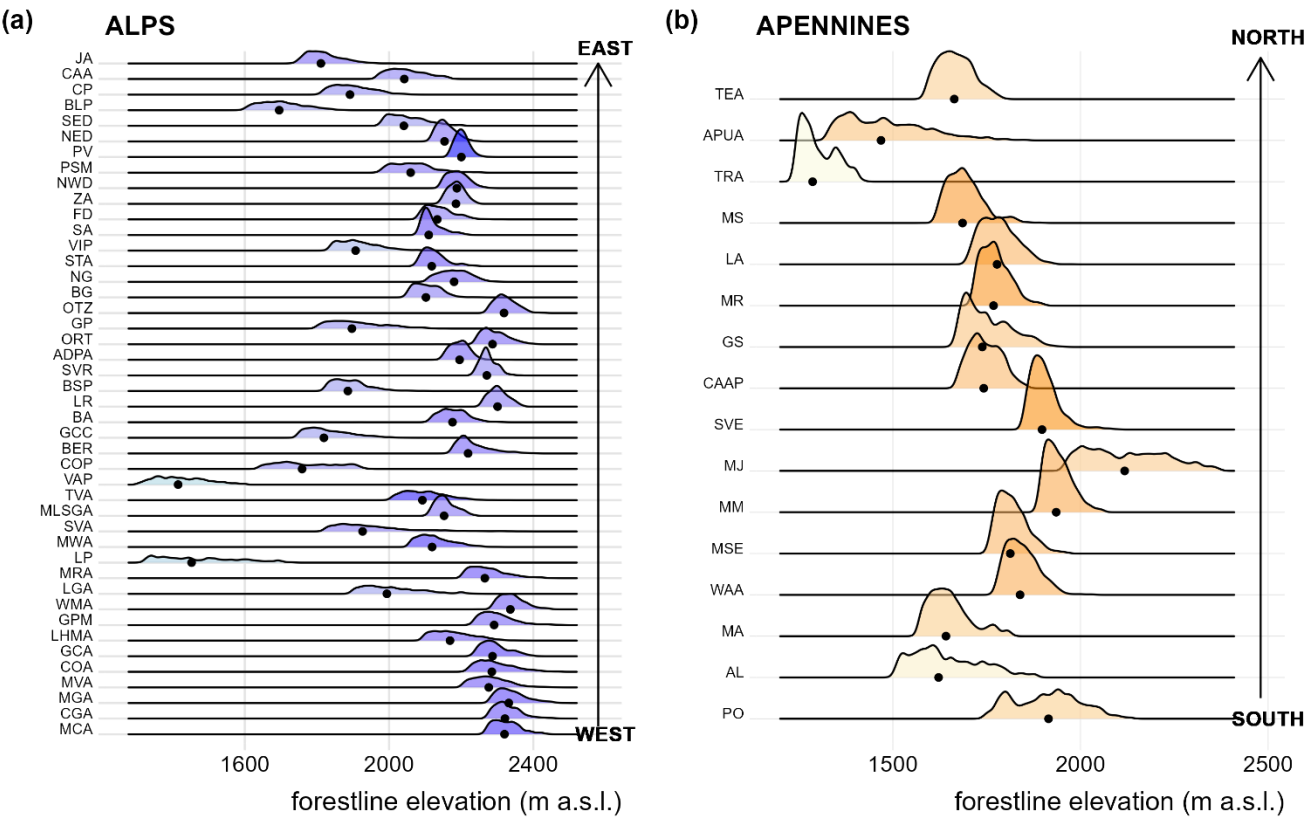


**Figure 4 - (a) Forestline elevation ranges of the mountain groups in the Alps (n = 44), sorted by longitude (West – East); (b) Forestline elevation ranges of the mountain groups of the Apennines (n = 16), sorted by latitude (South – North). Black dots is the median value of each interval5; colour intensity of ridges increases with forestline length and forested area ratio. Mountain groups codes are available in Table A1 (Appendix A).**

### 3.2. Trend analysis and performances

We obtained 28.81 % of highly significant ( $\alpha < 0.005$ ) trends pixels for greenness and 19.69 % for wetness, considering only pixels with concordant p-values on all of the forming indices. The majority of TAU values were positive (Fig. 5) at both index types, with respectively 97.8 % and 99.8 % in the Alps, and 96.3 % and 99.7 % in the Apennines.

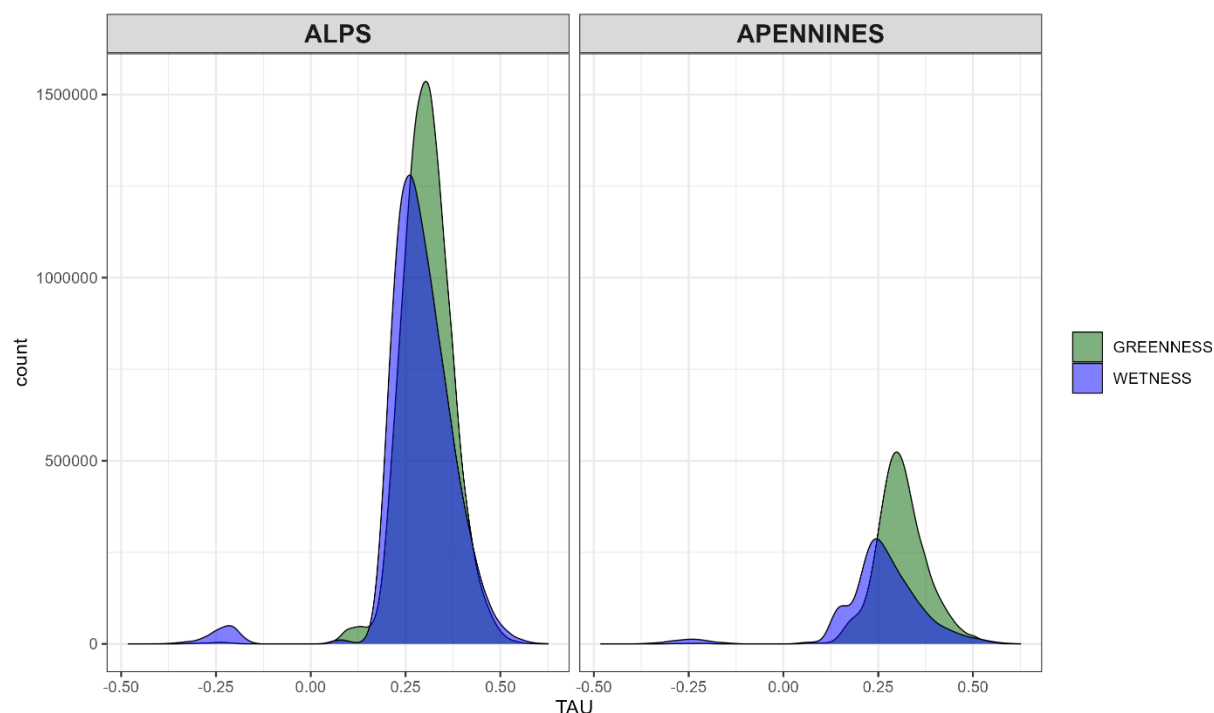


**Figure 5 – Distribution of the highly significant ( $\alpha < 0.005$ ) wetness (blue) and greenness (green) pixels frequency with different TAU values).**

245 In total, we obtained 242233 greenness and 221554 wetness highly significant positive trend pixels for the Alps, and 76348  
 and 508745 respectively for the Apennines. With sparse and moderate-to-dense canopy cover, the greenness and wetness  
 positive trends were mainly near the forestline in both mountain ranges, and decreased in both directions, but mainly upwards  
 where tree covered areas are gradually replaced by high-altitude grasslands. With dense canopy cover, only wetness positive  
 trends in the Apennines showed a similar distribution, differently from greenness trends and from both types in the Alps, where  
 250 the highest concentration was below and distant from the forestline (Fig. 6).

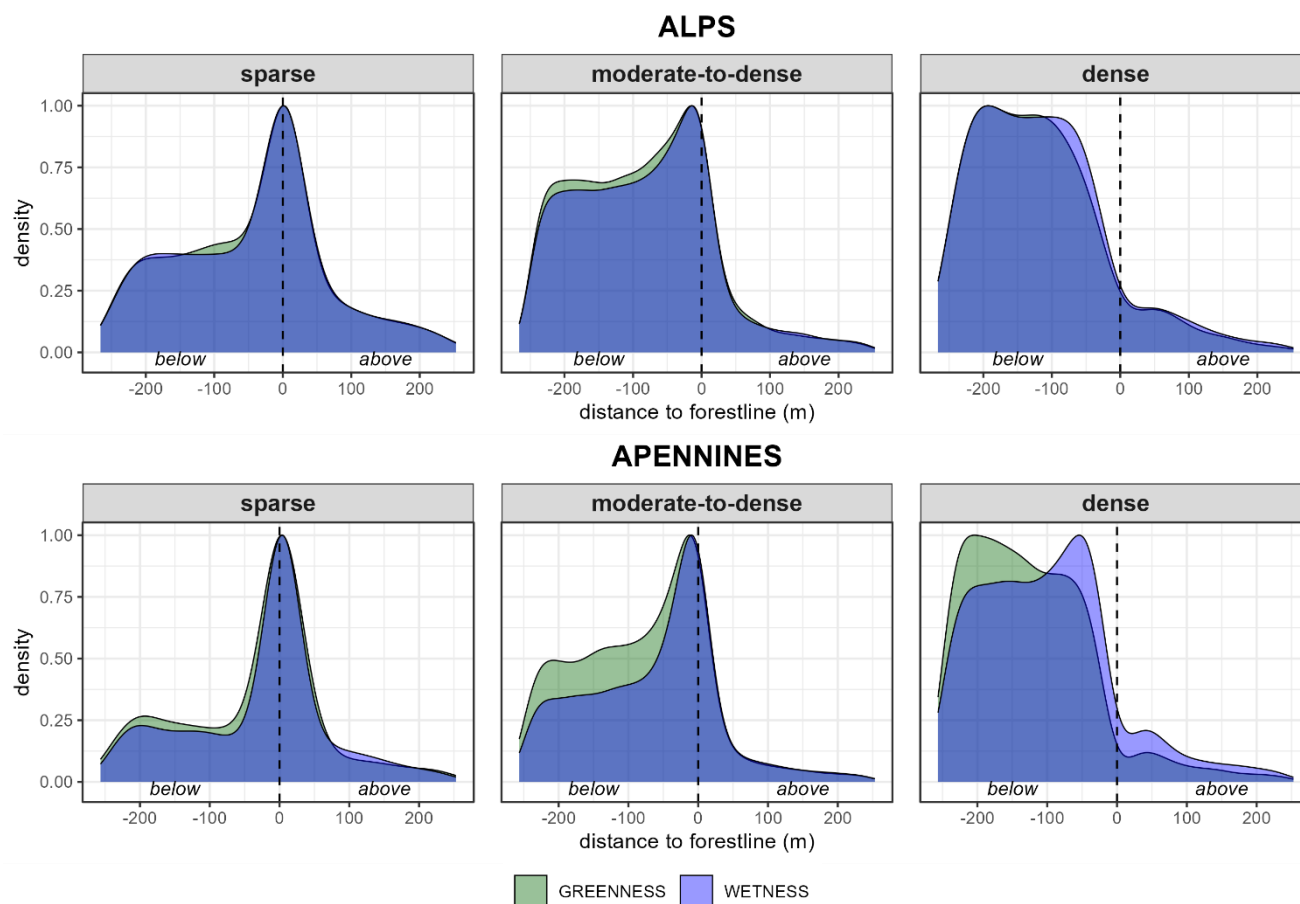


**Figure 6 – Positive wetness (blue) and greenness (green) trend pixels density according to their distance to the forestline (black dashed line) in different canopy cover classes: sparse (TCD < 10 %), moderate-to-dense (10 % < TCD < 80 %) and dense (TCD > 80%). Negative and positive values represent distances below and above the forestline, respectively.**

Significant differences between TAU trends and canopy cover classes occurred mainly in the Alps (Fig. 7). The highest ones were for the wetness indices in the dense canopy cover. For greenness, sparse canopy cover class had higher mean TAU than moderate-to-dense and dense classes. In the Apennines only greenness values highlighted a significant difference between the sparse and the dense canopy cover class.



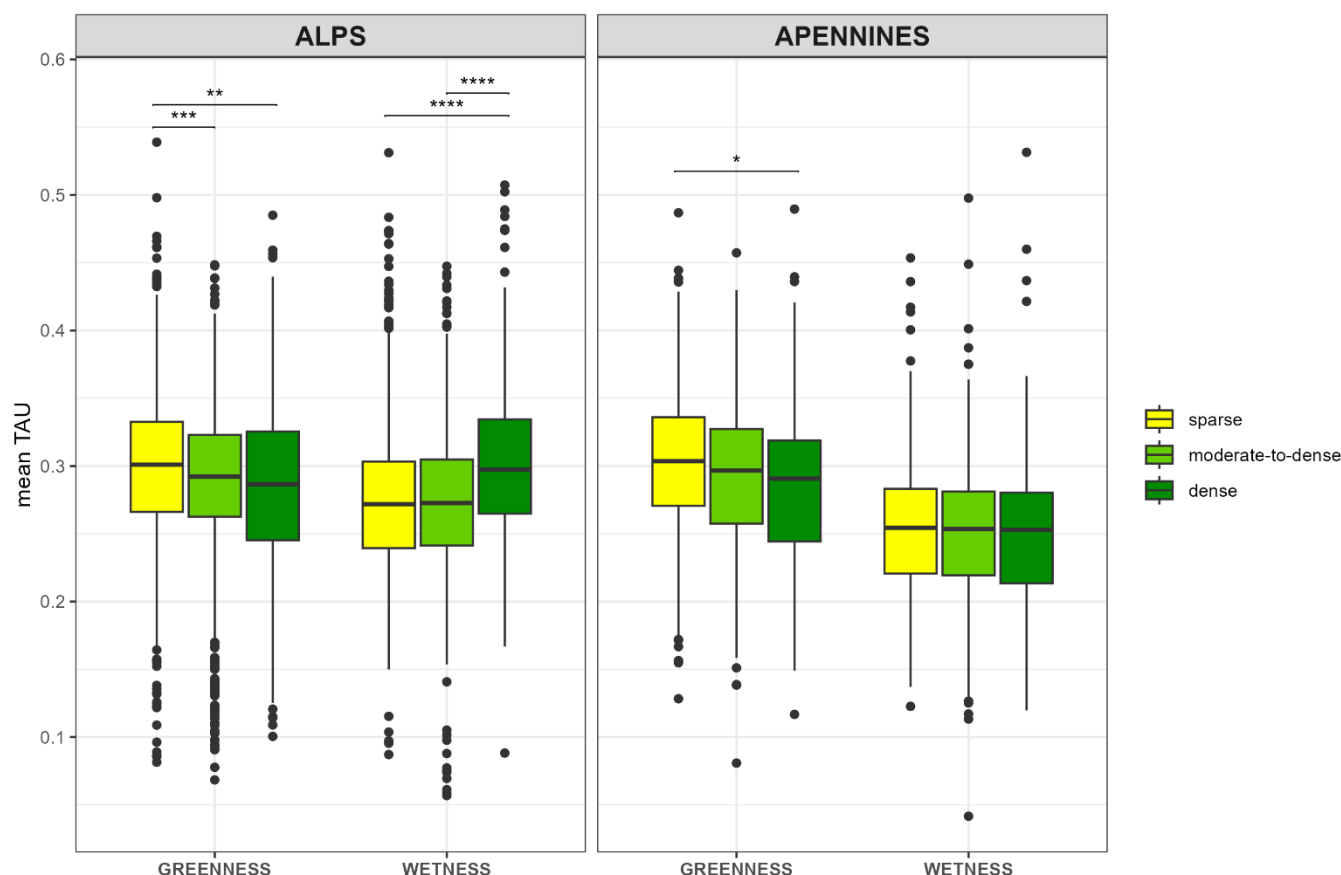


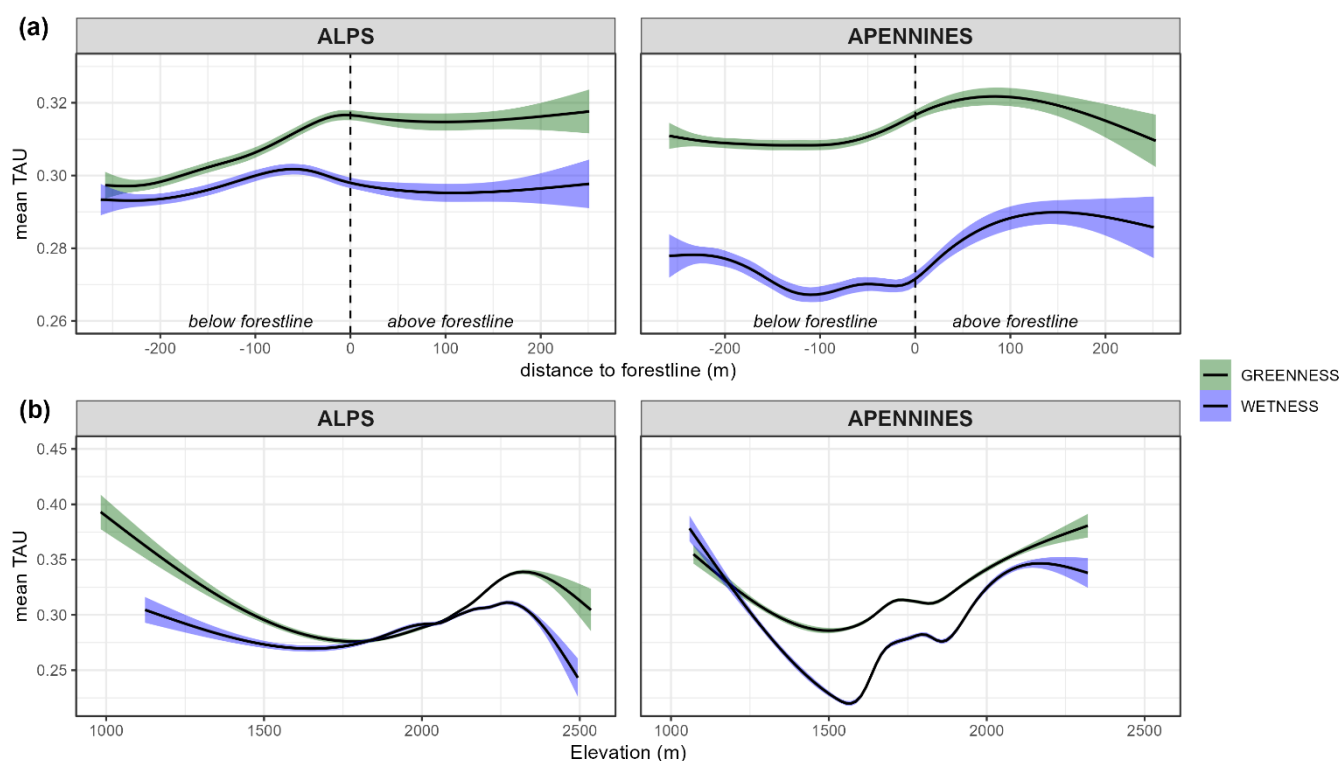
**Figure 7 – Boxplots of the mean TAU values of wetness and greenness trends in the Alps (left panel) and in the Apennines (right panel). The mean values in each forestline buffer account for three different canopy cover classes: sparse (yellow), moderate-to-dense (green), dense (dark green). Significant differences of Wilcoxon test are indicated with: \* ( $\alpha \leq 0.05$ ), \*\* ( $\alpha \leq 0.01$ ), \*\*\* ( $\alpha \leq 0.001$ ), \*\*\*\* ( $\alpha \leq 0.0001$ ). For more information on the canopy cover classes percentage in the Alps and in the Apennines refer to Fig. B1 (Appendix B).**

GAM models did not detect a statistically significant relationship between greenness/wetness mean TAU values, the distance to forestline, and the elevation (Fig. 8). Relatively similar patterns of the two indices mean trends appeared at both mountain ranges but with a higher variability in the Apennines. In general, TAU greenness values were higher than wetness ones. In the Alps, greenness increased moving upwards to the forestline with a first culmination close to and below it, followed by a decrease and subsequent increase, with the highest mean values over 200 m. In the Apennines instead, the mean TAU values increased close to the forestline with a culmination above it (about 100 m distance), followed by a decrease, with the lowest values above 200 m. In both the mountain ranges we observed a decrease of the greenness trends from lower elevations up to about 1750 m a.s.l. in the Alps and 1500 m a.s.l. in the Apennines (Fig. 8b). Thereafter, the mean TAU values increase



275 progressively in the Alps up to 2300 m a.s.l., but decrease slightly in the Apennines to around 1700 m a.s.l. to rise again up to the altitudinal limit.

Wetness trend related to the forestline distance is very flat in the Alps and relatively similar to that of the greenness, whereas in the Apennines, the trend is far more variable and increasing progressively from forestline up to 200 m above it (Fig. 8a). Wetness curves decrease for both Alps and Apennines from the lower elevations to about 1600 m a.s.l (Fig. 8b), with a more pronounced slope for the Apennines. Then they both rise up to about 2100 m a.s.l. with a steeper and fluctuating trend again in the Apennines.



285 **Figure 8 - Wetness (blue) and greenness (green) GAM functions with a level of confidence of 0.95, according to the elevation (a) and to the distance to the forestline (b) in the Alps (left) and in the Apennines (right). We considered the mean values of each forestline buffer. The models are not statistically significant ( $\alpha > 0.05$ ).**



## 4. Discussions

### 4.1. The uppermost forestlines detection method

The proposed forestline detection method is applicable at different spatial scales and in different geographic regions as it does not establish elevation thresholds and it can be based on regional datasets or other existing digital elevation models and forest masks. In addition, the method is also not exclusively based on climatic parameters, therefore applicable for the detection of human impacted forestlines. We considered as forestlines those closer to their potential climatic limit (e.g. tree species line), excluding forest margins at lower elevations and highly fragmented forestlines. We based the detection on the smallest elevation differences between the highest peaks and the forested pixels resulting from recent satellite derived data (TCD 2018). According to some authors, Italian and many others northern hemisphere forestlines are not “climatic” treelines due to severe human limitations (e.g. grazing, fire and deforestation) that altered altitudinal position, spatial pattern and tree composition (Motta et al., 2006; Malanson et al., 2011; Piermattei et al., 2016; Vitali et al., 2018; Holtmeier and Broll, 2020). In Italian mountains, forest upward expansion has been favoured mainly by past large-scale disturbances, and took place mainly at warmer aspects (Malandra et al., 2019). Recurrent human direct impacts on these ecotones since the Holocene times have greatly affected vegetation structure and composition (Foster et al., 1998), and recent silvo-pastoral abandonment at high elevation sites triggered secondary succession (Debussche et al., 1999). The different forest cover and the bioclimatic features of the selected mountain groups provide a representative sample of the forestline trends along the Italian peninsula. The mean forestlines elevations detected, confirm previous studies in the Alps (Caccianiga et al., 2008; Lingua et al., 2008; Diàz-Varela et al., 2010; Gilles et al., 2023) and in the Apennines (Vitali et al., 2018; Bonanomi et al., 2020). However, since the proposed method is closely dependent on the available regional/national datasets, some exclusion occurred with mountain groups at transnational borders.

### 4.2. Long-term greenness and wetness spectral trends

Overall, greenness and wetness raising trends were recorded at both mountain ranges in line with the ongoing natural reforestation processes (Vitali et al., 2018; Garbarino et al., 2020; Anselmetto et al., 2022). Pixel density distribution of Alps and Apennines are globally very similar, but some differences appear for the dense canopy cover class in the Apennines, where the wetness indices have the highest peak just below the forestline. This could be attributed to the different species composition at the two mountain ranges. Along the Apennines, with the exception of some scattered locations with *Pinus* spp., *Fagus sylvatica* is practically the only upper forestline species (Piermattei et al., 2014; Vitali et al., 2017). This would confirm the long term impact of human activity (Körner, 2012) and explain the occurrence of “abrupt” (Harsch et al., 2009) and static treelines (Bader et al., 2021; Bonanomi et al., 2018) given the very limited seed dispersal efficiency of beech (Vitali et al., 2017). Dominant species colonization rates, reproduction, seed-dispersal strategy and vitality of the occurring species are



320 relevant issues when comparing forestlines shifts in Alps and Apennines (Holtmeier, 2009; Compostella et al., 2017; Garbarino  
et al., 2020). In general gap-filling processes prevail at the deciduous Apennines forestlines (Malandra et al., 2019; Vitali et  
al., 2018), whereas in the Alps the coniferous species treeline (e.g. *Larix decidua*, *Pinus cembra* and *Picea abies*) foster tree  
encroachment at higher elevations. The beech regeneration (both by seeds and suckers) in the Apennines abrupt treelines have  
favoured processes of canopy thickening and gap filling below and near the forestline, better intercepted by wetness indices  
325 that are more sensitive to spectral response of the less exposed vegetation. Wetness indices are particularly sensitive to water  
content in both soil and plant especially in canopy leaf tissues. For this reason, we believe that significant increasing trends in  
areas with a dense canopy cover could be associated to crown thinning and biomass increase, as in gap filling, while in areas  
with sparse canopy cover, to new encroachment in open areas.

Considering the magnitude of changes rather than their frequency, in the Apennines we assessed a significant difference only  
330 for greenness mean TAU that resulted lower in dense than in sparse canopy cover conditions. We assume that the drier climatic  
conditions of the Apennines, may have influenced the positive trends of wetness indices, reducing the TAU variability in  
different canopy classes. The Wilcoxon test revealed the most significant variations in the Alps, where summer drought is not  
a limiting factor as in the Apennines. This hypothesis is confirmed by the higher mean TAU values of greenness in the sparse  
canopy class, whereas those of wetness refer to the dense one. Carlson et al. (2017) in the French Alps found a stronger  
335 greening signal in low-shrubs and open areas (e.g. grasslands or rocky habitats) than in forested areas. As well McManus et  
al. (2012) in the forest-tundra ecotones in Canada found higher greening in shrub and grass canopy classes. Sometimes, the  
greening of sparse open areas may be affected by melting glaciers (Rumpf et al., 2022), inducing a possible increase in soil  
moisture and influencing wetness trends too. Without considering the canopy cover class, the most relevant changes in the  
Apennines occurred above the forestline and at the lowest (< 1500 m a.s.l.) and highest (> 2000 m a.s.l.) elevations. Adding  
340 information about the forest structure could help identifying if the spectral signal sourced mostly from shrubs or newly  
established trees. In the Apennines, the highest mean TAU values above the forestline can be due to species like *Juniperus*  
*communis* L., *Pinus mugo* Turra and *Vaccinium myrtillus* L., that facilitate the upward migration of beech trees (Bonanomi et  
al., 2021). In the Alps, we found a steadier increase of TAU greenness and wetness from below to above the forestline. This  
confirms that diffuse treelines are more common in the Alps (Garbarino et al., 2020). Some authors used LiDAR data from the  
345 Global Ecosystem Dynamics Investigation (GEDI), integrated with Landast and Sentinel-2 data (Potapov et al., 2021; Tolan  
et al., 2024; Lang et al., 2023) to assess canopy height, vertical canopy structure and surface elevation, with the aim of  
monitoring forest ecosystems and carbon fluxes. This approach could be adopted in monitoring ecotones like treelines (Bolton  
et al., 2018), also to predict future vegetation scenarios and provide suitable management options (Morales-Molino et al.,  
2022).

350 Considering the greenness and wetness mean values of TAU trends only as a function of elevation, without the forestline  
distance information, their higher values are mainly at lower sites, where temperature is less limiting and the past human  
impact was greater (Malandra et al., 2019; Anselmetto et al., 2022). Furthermore forests at lower elevations are more accessible  
and usually most intensively managed in the past, but now are extensively abandoned (Malandra et al., 2019; Garbarino et al.,



2020). Above the mean forestline elevation of both Alps and Apennines, the mean TAU values increase and then decrease at  
355 higher altitudes where the number of pixels with significant increasing trends is also less. In the Apennines, a second short but  
clear decrease above 1750 m a.s.l. may depend on the frequent abrupt beech treelines where the forest margin is sharply  
separated from areas with sparse and different vegetation. This common trend for both mountain ranges confirms an upward  
recolonisation process at the Italian anthropogenic treelines. The decreasing magnitude observed at higher elevation with the  
increasing distance from the forestline is probably due to the larger distance from seed trees (Vitali et al., 2018), the more  
360 limiting effect of temperature and the synergic effect of topography and microclimate.

Uncertainty remains about causes of the spatial variability of trends, as noted also by Choler et al. (2021). The time-series span  
and the spatial resolution of satellite images are crucial aspects in the definition of this kind of ecological models. Nevertheless,  
the integration of different data sources (e.g. LiDAR) and the modelling of further environmental, climate and anthropogenic  
drivers can be essential for a better understanding of the current and future forestline dynamics.

## 365 5. Conclusions

This work introduced a new method to demarcate the upper forestlines at a regional scale, in environments where they do not  
match the climatic boundary (i.e. the 6 °C isotherm sensu Körner and Paulsen, 2004). We proposed several parameters to  
define only the forestlines closest to their potential position, detecting the ones nearest to mountain top with land cover and  
bioclimatic features. The use of TCD, with national or European digital terrain models, makes it applicable in most parts of  
370 Europe, but with similar datasets also in other regions of the world and at different scale of analysis. High spatial resolution,  
wide geographical coverage and open data availability policies are important factors for the replicability of the algorithm and  
for ensuring the quality of both the detection results and the trend analysis. Landsat images permit to analyse 40 year-long  
time-series with a suitable spatial resolution. Even though the two types of indices have different targets (greenness indices for  
photosynthetic activity and wetness indices for water content), the results were congruous and emphasized the altitudinal  
375 expansion of the forestline ecotone at national scale. Wetness indices were more sensitive in areas with denser canopy cover,  
probably due to gap-filling processes and increasing biomass. Greenness indices detected more relevant trends, especially in  
areas with sparse or medium canopy cover, probably where recent tree encroachment occurred in previously open areas.

In the current context of climate change and post-abandonment dynamics, the implementation of semi-automatic methods for  
detection and monitoring of vegetation spatial patterns and modelling of spectral trends is an added value. With this study, we  
380 defined hotspots of changes through different spectral indices and can be the basis for future landscape-scale analyses to better  
assess the relationships between climate, topography, vegetation dynamics and forest structure changes..





## 6. Appendices

### Appendix A:

385 **Table A1 - Selected Italian GMBA mountain groups, whose peaks having land cover and thermotypes suitable for the proposed algorithm. Elevation information was extracted from the Tinitaly DEM, limiting the areas to the national administrative boundaries.**

ID		Mountain group statistics				Forestline statistics						
Code	Name	highest peak (m)	min elevation (m)	forested area (km <sup>2</sup> )	area (km <sup>2</sup> )	length (km)	mean length (km)	n°	mean elevation (m)	median elevation (m)	max elevation (m)	Length/forested area (km km <sup>-2</sup> )
<b>ALPS</b>												
<b>ADPA</b>	Adamello-Presanella Alps	3552	250	657	1379	115	0.98 ± 0.56	118	2196 ± 27	2196	2343	0.175
<b>BA</b>	Bergamasque Alps	3030	198	815	1417	151	1.06 ± 0.74	146	2179 ± 39	2176	2332	0.185
<b>BER</b>	Bernina Range	3998	0	431	976	76	1.13 ± 0.78	67	2233 ± 46	2219	2416	0.176
<b>BG</b>	Brenta group	3163	190	455	706	68	1.19 ± 0.97	57	2107 ± 37	2102	2272	0.149
<b>BLP</b>	Bellunese Prealps	2457	26	1058	1494	128	1.76 ± 2.62	73	1701 ± 60	1695	1889	0.121
<b>BSP</b>	Brescia Prealps	2250	125	811	1124	96	2.16 ± 1.59	44	1892 ± 48	1886	2109	0.118
<b>CAA</b>	Carnic Alps	2778	241	1202	1720	173	1.36 ± 1.38	92	2049 ± 51	2042	2193	0.144
<b>CGA</b>	Central Graian Alps	3747	660	136	619	26	1.09 ± 0.6	24	2329 ± 37	2321	2479	0.191
<b>COA</b>	Cottian Alps	3286	0	345	823	69	1.08 ± 0.67	64	2295 ± 51	2285	2481	0.2
<b>COP</b>	Como Prealps	2242	0	569	847	78	3.12 ± 3.62	25	1773 ± 82	1759	1950	0.137
<b>CP</b>	Carnic Prealps	2703	132	933	1304	125	2.21 ± 3.1	78	1899 ± 55	1892	2092	0.134
<b>FD</b>	Fiemme Dolomites	2844	186	1445	1971	219	1.56 ± 1.4	141	2140 ± 40	2134	2326	0.151
<b>GCA</b>	Grand Combin Alps	3725	555	141	538	29	1.14 ± 0.8	82	2293 ± 38	2287	2420	0.206
<b>GCC</b>	Gruppo Camino-Concarena	2547	158	1373	2003	164	1.51 ± 1.62	106	1833 ± 63	1819	2126	0.119
<b>GP</b>	Garda Prealps	2251	12	1273	1686	168	1.87 ± 1.72	90	1911 ± 76	1897	2163	0.132
<b>GPM</b>	Grand Paradis Massif	4060	236	537	1563	93	1.01 ± 0.61	29	2299 ± 45	2291	2491	0.174
<b>JA</b>	Julian Alps	2751	311	286	439	48	1.17 ± 0.64	41	1819 ± 47	1811	2017	0.168
<b>LGA</b>	Ligurian Alps	2650	0	1503	2051	169	1.88 ± 1.58	90	2008 ± 78	1994	2262	0.112



<b>LHMA</b>	Lanzo and Haute Maurienne Alps	3676	0	611	1291	114	$1.5 \pm 1.5$	76	$2177 \pm 56$	2169	2387	0.186
<b>LP</b>	Ligurian Prealps	1743	0	875	1043	50	$2.65 \pm 5.04$	19	$1474 \pm 109$	1452	1743	0.057
<b>LR</b>	Livigno Range	3436	0	180	630	28	$1.01 \pm 0.64$	26	$2303 \pm 26$	2301	2376	0.153
<b>MCA</b>	Mont Cenis Alps	3468	515	126	352	27	$0.84 \pm 0.6$	26	$2325 \pm 37$	2320	2444	0.216
<b>MGA</b>	Montgenevre Alps	3301	277	797	1432	159	$1.31 \pm 1.21$	121	$2339 \pm 41$	2332	2500	0.2
<b>MLSGA</b>	Mont Leone and Saint Gothard Alps	3551	0	132	379	21	$1.51 \pm 1.13$	18	$2157 \pm 28$	2153	2245	0.159
<b>MRA</b>	Monte Rosa Alps	4607	197	584	1382	113	$1.75 \pm 1.38$	110	$2275 \pm 51$	2266	2469	0.194
<b>MVA</b>	Monte Viso Alps	3841	275	1041	1971	192	$1.32 \pm 1.28$	86	$2282 \pm 50$	2277	2486	0.185
<b>MWA</b>	Mischabel and Weissmies Alps	3610	223	194	392	42	$1.02 \pm 0.58$	41	$2127 \pm 48$	2119	2313	0.216
<b>NED</b>	Northeastern Dolomites	3261	529	744	1474	118	$1.11 \pm 0.72$	108	$2158 \pm 26$	2154	2253	0.159
<b>NG</b>	Nonsberg Group	2953	200	693	966	119	$1.61 \pm 1.33$	72	$2181 \pm 41$	2180	2319	0.172
<b>NWD</b>	Northwest Dolomites	3343	276	803	1426	156	$1.11 \pm 0.74$	141	$2190 \pm 29$	2188	2298	0.194
<b>ORT</b>	Ortler Alps	3892	270	715	1768	123	$1.28 \pm 0.9$	99	$2293 \pm 36$	2287	2419	0.172
<b>OTZ</b>	Ötztal Alps	3723	0	300	1024	51	$0.97 \pm 0.61$	53	$2323 \pm 30$	2319	2438	0.171
<b>PSM</b>	Pale di San Martino	3190	260	456	742	74	$1.8 \pm 2.05$	40	$2064 \pm 55$	2060	2263	0.161
<b>PV</b>	Puster Valley	3424	807	257	531	61	$1.08 \pm 0.7$	56	$2202 \pm 19$	2200	2288	0.236
<b>SA</b>	Sarntal Alps	2773	239	654	1115	124	$1.28 \pm 0.86$	97	$2119 \pm 29$	2110	2245	0.19
<b>SED</b>	Southeast Dolomites	3217	351	446	659	54	$1.52 \pm 1.09$	34	$2050 \pm 51$	2041	2217	0.12
<b>STA</b>	Stubai Alps	3454	675	123	355	23	$1.01 \pm 0.66$	23	$2125 \pm 34$	2118	2251	0.189
<b>SVA</b>	Southern Valais Alps	2590	193	995	1412	155	$2.34 \pm 2.31$	66	$1953 \pm 105$	1927	2396	0.156
<b>SVR</b>	Sesvenna Range	3174	0	120	359	17	$0.96 \pm 0.43$	19	$2275 \pm 22$	2271	2370	0.141
<b>TVA</b>	Ticino and Verbano Alps	3272	192	603	898	138	$1.58 \pm 1.48$	87	$2098 \pm 57$	2093	2335	0.229
<b>VAP</b>	Varese Prealps	1648	0	313	410	16	$2.31 \pm 2.44$	7	$1424 \pm 70$	1417	1603	0.052



<b>VIP</b>	Vicentine Prealps	2333	34	1916	2843	175	$2.24 \pm 3.66$	78	$1917 \pm 57$	1907	2135	0.091
<b>WMA</b>	Weissshorn and Matterhorn Alps	4470	448	122	424	22	$0.97 \pm 0.72$	23	$2340 \pm 35$	2336	2458	0.183
<b>ZA</b>	Zillertal Alps	3499	563	381	863	52	$0.81 \pm 0.31$	64	$2186 \pm 22$	2186	2249	0.136
<b>APENNINES</b>												
<b>AL</b>	Alburni	1897	0	1699	2277	43	$3.09 \pm 3.2$	14	$1643 \pm 91$	1622	1886	0.025
<b>APUA</b>	Apuan Alps	1937	0	965	1224	96	$2.34 \pm 3$	41	$1484 \pm 111$	1468	1864	0.099
<b>CAAP</b>	Central Abruzzi Apennines	1999	387	559	887	65	$2.61 \pm 3.44$	22	$1746 \pm 42$	1742	1862	0.117
<b>GS</b>	Gran Sasso	2908	90	815	1795	80	$1.86 \pm 1.48$	43	$1751 \pm 61$	1738	1964	0.098
<b>LA</b>	Laga	2457	90	1066	1662	132	$3.15 \pm 4.27$	42	$1782 \pm 48$	1778	1989	0.124
<b>MA</b>	Matese	2049	60	810	1211	67	$2.58 \pm 2.66$	26	$1651 \pm 56$	1641	1820	0.083
<b>MJ</b>	Majella	2792	98	766	1344	65	$2.25 \pm 3.83$	29	$2124 \pm 106$	2118	2383	0.085
<b>MM</b>	Monti Marsicani	2284	325	507	943	72	$1.63 \pm 1.77$	44	$1941 \pm 35$	1935	2066	0.142
<b>MR</b>	Monti Reatini	2214	369	275	389	47	$1.63 \pm 1.12$	29	$1773 \pm 38$	1768	1906	0.172
<b>MS</b>	Monti Sibillini	2476	239	409	871	68	$1.89 \pm 2.11$	36	$1692 \pm 48$	1686	1902	0.166
<b>MSE</b>	Monti Simbruini-Ernici	2155	223	811	1034	98	$2.57 \pm 2.28$	38	$1818 \pm 40$	1813	1977	0.12
<b>PO</b>	Pollino	2265	0	1287	3326	107	$6.66 \pm 11.52$	16	$1910 \pm 88$	1915	2147	0.083
<b>SVE</b>	Sirente Velino	2484	248	426	1069	78	$1.62 \pm 1.56$	53	$1904 \pm 39$	1897	2101	0.182
<b>TEA</b>	Tuscan Emilian Apennines	2163	20	4387	6245	345	$2.85 \pm 5.46$	121	$1667 \pm 45$	1664	1808	0.079
<b>TRA</b>	Tosco Romagnolo Apennines	1654	47	3954	5659	28	$1.85 \pm 2.01$	15	$1301 \pm 47$	1286	1427	0.007
<b>WAA</b>	Western Abruzzi Apennines	2247	35	1142	1664	154	$2.49 \pm 2.62$	62	$1844 \pm 43$	1839	2045	0.135





## 9. Authors contribution

LB: methodology, formal analysis, data curation and writing; DM: methodology, supervision, formal analysis, investigation, writing—review and editing; MG: conceptualization, methodology, investigation, funding acquisition, supervision, writing—review and editing; CU: conceptualization, writing—review and editing; EL: writing—review and editing; RM: writing—  
405 review and editing; AV: Conceptualization, supervision, methodology, writing—review and editing.

## 10. Competing interests

Matteo Garbarino is guest editor of the special issue “Treeline ecotones under global change: linking spatial patterns to ecological processes” in Biogeosciences.

## 11. Acknowledgments

410 This research was cofunded by the European Union – NextGeneration EU, Mission 4, Component 1 (CUP I53D23003180006 - PRIN - 2022 OLYMPUS - Spatio-temporal analysis of Mediterranean treeline patterns: a multiscale approach).

## 12. References

- Ameztegui, A., Coll, L., Brotons, L., and Ninot, J. M. . Land-use legacies rather than climate change are driving the recent upward shift of the mountain tree line in the Pyrenees. *Global Ecology and Biogeography*, 25(3), 263–273. doi: 10.1111/geb.12407, 2016.
- 415 Anselmetto, N., Sibona, E. M., Meloni, F., Gagliardi, L., Bocca, M., and Garbarino, M. . Land Use Modeling Predicts Divergent Patterns of Change Between Upper and Lower Elevations in a Subalpine Watershed of the Alps. *Ecosystems*, 25, 1295–1310. doi: 10.1007/s10021-021-0071, 2022.
- Arekhi, M., Yesil, A., Ozkan, U. Y., and Balik Sanli, F. . Detecting treeline dynamics in response to climate warming using forest stand maps and Landsat data in a temperate forest. *Forest Ecosystems*, 5(1). doi:10.1186/s40663-018-0141-3, 2018
- 420 Bader, M. Y., Llambí, L. D., Case, B. S., Buckley, H. L., Toivonen, J. M., Camarero, J. J., Cairns, D. M., Brown, C. D., Wiegand, T., and Resler, L. M. . A global framework for linking alpine-treeline ecotone patterns to underlying processes. *Ecography*, 44(2), 265–292. doi: 10.1111/ecog.05285, 2021
- Bayle, A., Gascoin, S., Berner, L. T., and Choler, P. . Landsat-based greening trends in alpine ecosystems are inflated by multidecadal increases in summer observations. *Ecography*. doi: 10.1111/ecog.07394, 2024.
- 425 Bayle, A., Nicoud, B., Mansons, J., Francon, L., Corona, C., and Choler, P. . Alpine greening deciphered by forest stand and structure dynamics in advancing treelines of the southwestern European Alps. *Remote Sensing in Ecology and Conservation*. <https://doi.org/10.1002/rse2.430>, 2025.
- Bengtsson, H. A Unifying Framework for Parallel and Distributed Processing in R using Futures, *The R Journal* 13:2, 208–227, doi:10.32614/RJ-2021-048, 2021.
- 430 Berdanier, A., . Global treeline position. *Nature Education Knowledge* 3: 11–19, 2010.
- Bharti, R. R., Adhikari, B. S., and Rawat, G. S. Assessing vegetation changes in timberline ecotone of Nanda Devi National Park, Uttarakhand. *International Journal of Applied Earth Observation and Geoinformation*, 18(1), 472–479. <https://doi.org/10.1016/j.jag.2011.09.018>, 2012.





- 435 Blasi, C., Capotorti, G., Copiz, R., Guida, D., Mollo, B., Smiraglia, D., Zavattero, L. . Classification and mapping of the  
ecoregions of Italy. *Plant Biosystems*. 10.1080/11263504.2014.985756, 2014.
- Bolton, D. K., Coops, N. C., Hermosilla, T., Wulder, M. A., and White, J. C..Evidence of vegetation greening at alpine treeline  
ecotones: Three decades of Landsat spectral trends informed by lidar-derived vertical structure. *Environmental Research*  
*Letters*, 13(8). doi: 10.1088/1748-9326/aad5d2, 2018.
- 440 Bonanomi, G., Mogavero, V., Rita, A., Zotti, M., Saulino, L., Tesei, G., et al. Shrub facilitation promotes advancing of  
the *Fagus sylvatica* treeline across the Apennines (Italy). *Journal of Vegetation Science*, 32:  
e13054. <https://doi.org/10.1111/jvs.13054>, 2021.
- Bonanomi, G., Rita, A., Allevato, E., Cesarano, G., Saulino, L., di Pasquale, G., Allegrezza, M., Pesaresi, S., Borghetti, M.,  
Rossi, S., and Saracino, A... Anthropogenic and environmental factors affect the tree line position of *Fagus sylvatica*  
along the Apennines (Italy). *Journal of Biogeography*, 45(11), 2595–2608. <https://doi.org/10.1111/jbi.13408>, 2018.
- 445 Bonanomi, G., Zotti, M., Mogavero, V., Cesarano, G., Saulino, L., Rita, A., Tesei, G., Allegrezza, M., Saracino, A., and  
Allevato, E..Climatic and anthropogenic factors explain the variability of *Fagus sylvatica* treeline elevation in fifteen  
mountain groups across the Apennines. *Forest Ecosystems*, 7(1). doi: 10.1186/s40663-020-0217-8, 2020.
- Brown, F. C., Brumby, S. P., Guzder-Williams, B., Birch, T., Hyde, S., Mazzariello, J., . . . Moore, R. . Dynamic World, Near  
real-time global 10 m land use land cover mapping. *Scientific Data*, 9(1), 251, 2022.
- 450 Caccianiga, M., Andreis, C., Armiraglio, S., Leonelli, G., Pelfini, M., Sadla, D..Climate continentality and treeline species  
distribution on the Alps. *Plant Bios* 142, 66–78, 2008.
- Camps-Valls, G., Campos-Taberner, M., Moreno-Martinez, A., Walther, S., Duveiller, G., Cescatti, A. et al. A unified  
vegetation index for quantifying the terrestrial biosphere. *Science Advances*, 7(9).  
455 <https://doi.org/10.1126/sciadv.abc7447>, 2021.
- Carlson, B. Z., Corona, M. C., Dentant, C., Bonet, R., Thuiller, W., and Choler, P. . Observed long-term greening of alpine  
vegetation - A case study in the French Alps. *Environmental Research Letters*, 12(11). <https://doi.org/10.1088/1748-9326/aa84bd>, 2017.
- Choler, P., Bayle, A., Carlson, B. Z., Randin, C., Filippa, G., and Cremonese, E. . The tempo of greening in the European Alps:  
Spatial variations on a common theme. *Global Change Biology*, 27(21), 5614–5628. doi: 10.1111/gcb.15820, 2021.
- 460 Chhetri, P. K., and Thai, E.. Remote sensing and geographic information systems techniques in studies on treeline ecotone  
dynamics. In *Journal of Forestry Research* (Vol. 30, Issue 5, pp. 1543–1553). Northeast Forestry University.  
<https://doi.org/10.1007/s11676-019-00897-x>, 2019.
- Choler, P., Bayle, A., Carlson, B. Z., Randin, C., Filippa, G., and Cremonese, E..The tempo of greening in the European Alps:  
Spatial variations on a common theme. *Global Change Biology*, 27(21), 5614–5628. <https://doi.org/10.1111/gcb.15820>,  
465 2021.
- Choler, P., Bayle, A., Fort, N. Gascoin, S. Waning snowfields have transformed into hotspots of greening within the alpine  
zone. *Nature Climate Change*. <https://doi.org/10.1038/s41558-024-02177-x>, 2024.
- Cohen, W. B., and Goward, S. . Landsat's role in ecological applications of remote sensing. *Bioscience*, 54, 535–545., 2004.
- 470 Cohen W.B., Spies T., Fiorella M. . Estimating the age and structure of forests in a multi-ownership landscape of western  
Oregon, U.S.A. *International Journal of Remote Sensing* 16: 721–746., 1995.
- Compostella, C., and Caccianiga, M.. A comparison between different treeline types shows contrasting responses to climate  
fluctuations. *Plant Biosystems*, 151(3), 436–449. doi: 10.1080/11263504.2016.1179695, 2017.
- Copernicus Land Monitoring Service,High Resolution land cover characteristics Tree-cover/forest and change 2015-2018.  
User manual. European Environment Agency (EEA), 2021.
- 475 Crist, E. P. A TM Tasseled Cap equivalent transformation for reflectance factor data. *Remote Sensing of Environment*, 17(3),  
301–306. doi: 10.1016/0034-4257(85)90102-6, 1985.
- Crist, E. P., and Cicone, R. C. A Physically-Based Transformation of Thematic Mapper Data-The TM Tasseled Cap. In *IEEE*  
*TRANSACTIONS ON GEOSCIENCE AND REMOTE SENSING* (Issue 3), 1984.
- 480 Csárdi G. and Chang W. callr: Call R from R. R package version 3.7.6, <https://CRAN.R-project.org/package=callr>, 2024.
- Debussche, M., Lepart, J., and Dervieux, A. Mediterranean landscape changes: Evidence from old postcards. *Global Ecology*  
and *Biogeography*, 8(1), 3–15. doi: 10.1046/j.1365-2699.1999.00316.x, 1999.



- Diáz-Varela, R. A., Colombo, R., Meroni, M., Calvo\_Iglesias, M., S., Buffoni, A., Tagliaferri, A.. Spatio-temporal analysis of  
alpine ecotones: A spatial explicit model targeting altitudinal vegetation shifts. *Ecological Modelling*, 221(4), 621–633.  
doi: [doi.org/10.1016/j.ecolmodel.2009.11.010](https://doi.org/10.1016/j.ecolmodel.2009.11.010), 2010.
- Dziomber, L., Gobet, E., Leunda, M., Gurtner, L., Vogel, H., Tournier, N., Damanik, A., Szidat, S., Tinner, W., and Schwörer,  
C.. Palaeoecological multiproxy reconstruction captures long-term climatic and anthropogenic impacts on vegetation  
dynamics in the Rhaetian Alps. *Review of Palaeobotany and Palynology*, 321, 105020. doi:  
[10.1016/J.REVPALBO.2023.105020](https://doi.org/10.1016/J.REVPALBO.2023.105020), 2024.
- FAO. Global Forest Resources Assessment (FRA), 2000.
- Fauquette, S., Suc, J.-P., Médail, F., Muller, S. D., Jiménez-Moreno, G., Bertini, A., Martinetto, E., Popescu, S. M., Zheng,  
Z., and de Beaulieu, J.-L.. The Alps: A Geological, Climatic and Human Perspective on Vegetation History and Modern  
Plant Diversity. <https://amu.hal.science/hal-01888883>, 2018.
- Fissore, V., Motta, R., Palik, B., and Mondino, E. B.. The role of spatial data and geomatic approaches in treeline mapping: A  
review of methods and limitations. *European Journal of Remote Sensing*, 48, 777–792.  
<https://doi.org/10.5721/EuJRS20154843>, 2015.
- Flood, N.. Seasonal Composite Landsat TM/ETM+ Images Using the Medoid (a Multi-Dimensional Median). *Remote Sensing*,  
5(12), 6481–6500. <https://doi.org/10.3390/rs5126481>, 2013.
- Foster, D. R., Motzkin, G., and Slater, B. Land-Use History as Long-Term Broad-Scale Disturbance: Regional Forest Dynamics  
in Central New England. Gao, B. C. (1996). NDWI—A normalized difference water index for remote sensing of  
vegetation liquid water from space. *Remote Sensing of Environment*, 58(3), 257–266. doi: 10.1016/S0034-  
4257(96)00067-3, 1998.
- Gao, B.-C.. NDWI - A normalized difference water index for remote sensing of vegetation liquid water from space. *Remote  
Sensing of Environment* 58: 257–266, 1996.
- Garbarino, M., Morresi, D., Anselmetto, N., and Weisberg, P. J.. Treeline remote sensing: from tracking treeline shifts to multi-  
dimensional monitoring of ecotonal change. In *Remote Sensing in Ecology and Conservation* (Vol. 9, Issue 6, pp. 729–  
742). John Wiley and Sons Inc. doi: 10.1002/rse2.351, 2023.
- Garbarino, M., Morresi, D., Urbinati, C., Malandra, F., Motta, R., Sibona, E. M., Vitali, A., and Weisberg, P. J.. Contrasting  
land use legacy effects on forest landscape dynamics in the Italian Alps and the Apennines. *Landscape Ecology*, 35(12),  
2679–2694. doi: [10.1007/s10980-020-01013-9](https://doi.org/10.1007/s10980-020-01013-9), 2020.
- García, M. J. L., and Caselles, V.. Mapping burns and natural reforestation using thematic mapper data. *Geocarto International*,  
6(1), 31–37. doi: [10.1080/10106049109354290](https://doi.org/10.1080/10106049109354290), 1991.
- Gilles, A., Lavergne, S., and Carcaillet, C.. Unsuspected prevalence of *Pinus cembra* in the high-elevation sky islands of the  
western Alps. *Plant Ecology*, 224(10), 865–873. <https://doi.org/10.1007/s11258-023-01341-1>, 2023.
- Gómez, C., White, J. C., and Wulder, M. A.. Characterizing the state and processes of change in a dynamic forest environment  
using hierarchical spatio-temporal segmentation. *Remote Sensing of Environment*, 115(7), 1665–1679. doi:  
[10.1016/j.rse.2011.02.025](https://doi.org/10.1016/j.rse.2011.02.025), 2011.
- Gómez, C., White, J. C., and Wulder, M. A. . Optical remotely sensed time series data for land cover classification: A review.  
*ISPRS Journal of Photogrammetry and Remote Sensing*, 116, 55–72. doi: [10.1016/J.ISPRSJPRS.2016.03.008](https://doi.org/10.1016/J.ISPRSJPRS.2016.03.008), 2016.
- Hansson, A., Dargusch, P., and Shulmeister, J.. A Review of Methods Used to Measure Treeline Migration and Their  
Application. In *Journal of Environmental Informatics Letters* (Vol. 4, Issue 1, pp. 1–10). International Society for  
Environmental Information Sciences. doi: [10.3808/jeil.202000037](https://doi.org/10.3808/jeil.202000037), 2020.
- Hansson, A., Yang, W. H., Dargusch, P., and Shulmeister, J.. Investigation of the Relationship Between Treeline Migration and  
Changes in Temperature and Precipitation for the Northern Hemisphere and Sub-regions. In *Current Forestry Reports*  
(Vol. 9, Issue 2, pp. 72–100). Springer Science and Business Media Deutschland GmbH. doi: [10.1007/s40725-023-00180-7](https://doi.org/10.1007/s40725-023-00180-7), 2023.
- Harsch, M. A., and Bader, M. Y.. Treeline form - a potential key to understanding treeline dynamics. *Global Ecology and  
Biogeography*, 20(4), 582–596. doi: [10.1111/j.1466-8238.2010.00622.x](https://doi.org/10.1111/j.1466-8238.2010.00622.x), 2011.
- He, X., Jiang, X., Spracklen, D. v., Holden, J., Liang, E., Liu, H., Xu, C., Du, J., Zhu, K., Elsen, P. R., and Zeng, Z.. Global  
distribution and climatic controls of natural mountain treelines. *Global Change Biology*, 29(24), 7001–7011.  
<https://doi.org/10.1111/gcb.16885>Hastie, T. J.; Tibshirani, R. J. (1990). *Generalized Additive Models*. Chapman &  
Hall/CRC. [ISBN 978-0-412-34390-2](https://doi.org/10.1111/gcb.16885), 2023.



- Hijmans, R.. terra: Spatial Data Analysis. R package version 1.7-55. Tratto da <https://CRAN.R-project.org/package=terra>, 2023.
- 535 Holtmeier, F.K.. Mountain Timberlines. *Advances in Global Change Research*, vol 36. Springer, Dordrecht. [https://doi.org/10.1007/978-1-4020-9705-8\\_1](https://doi.org/10.1007/978-1-4020-9705-8_1), 2009.
- Holtmeier, F. K., and Broll, G.. Sensitivity and response of northern hemisphere altitudinal and polar treelines to environmental change at landscape and local scales. *Global Ecology and Biogeography*, 14(5), 395–410. doi: 10.1111/j.1466-822X.2005.00168.x, 2005.
- 540 Holtmeier, F. K., and Broll, G.. Treeline research-from the roots of the past to present time. a review. In *Forests* (Vol. 11, Issue 1). MDPI AG. doi: 10.3390/f11010038, 2020.
- Huete, A. R.. Vegetation Indices, Remote Sensing and Forest Monitoring. *Geography Compass*, 6(9), 513–532. <https://doi.org/10.1111/j.1749-8198.2012.00507.x>, 2012.
- 545 Huete, A., Didan, K., Miura, T., Rodriguez, E. P., Gao, X., and Ferreira, L. G.. Overview of the radiometric and biophysical performance of the MODIS vegetation indices. *Remote Sensing of Environment*, 83(1–2), 195–213. doi: 10.1016/S0034-4257(02)00096-2, 2002.
- Isotta, F. A., Frei, C., Weilguni, V., Perčec Tadić, M., Lassègues, P., Rudolf, B., Pavan, V., Cacciamani, C., Antolini, G., Ratto, S. M., Munari, M., Micheletti, S., Bonati, V., Lussana, C., Ronchi, C., Panettieri, E., Marigo, G., and Vertačnik, G.. The climate of daily precipitation in the Alps: Development and analysis of a high-resolution grid dataset from pan-Alpine rain-gauge data. *International Journal of Climatology*, 34(5), 1657–1675. <https://doi.org/10.1002/joc.3794>, 2014.
- 550 Kauth R. J. and G. S. Thomas: The Tasseled Cap - A Graphic Description of the Spectral-Temporal Development of Agricultural Crops as Seen by LANDSAT. *Proceedings of the Symposium on Machine Processing of Remotely Sensed Data*, 1976.
- Körner, C., Alpine Ecosystems and the High-Elevation Treeline. Sven Erik Jørgensen, Brian D. Fath, *Encyclopedia of Ecology*, Academic Press, 138-144. <https://doi.org/10.1016/B978-008045405-4.00314-1>, 2008.
- 555 Körner, C., Alpine Treelines. *Functional Ecology of the Global High Elevation Tree Limits*. Springer., 2012.
- Körner, C., and Paulsen, J.. A world-wide study of high altitude treeline temperatures. *Journal of Biogeography*, 31(5), 713–732. doi: 10.1111/j.1365-2699.2003.01043.x, 2004.
- 560 Kumar, R., Nath, A. J., Nath, A., Sahu, N., and Pandey, R.. Landsat-based multi-decadal spatio-temporal assessment of the vegetation greening and browning trend in the Eastern Indian Himalayan Region. *Remote Sensing Applications: Society and Environment*, 25. doi: 10.1016/j.rsase.2022.100695, 2022.
- Lang, N., Jetz, W., Schindler, K., and Wegner, J. D.. A high-resolution canopy height model of the Earth. *Nature Ecology and Evolution*, 7(11), 1778–1789. <https://doi.org/10.1038/s41559-023-02206-6>, 2023.
- 565 Leonelli, G., Pelfini, M., and Di Cella, U.. Detecting climatic treelines in the Italian alps: The influence of geomorphological factors and human impacts. *Physical Geography*, 30(4), 338–352. doi: 10.2747/0272-3646.30.4.338, 2009.
- Lingua, E., Cherubini, P., Motta, R., Nola, P. Spatial structure along an altitudinal gradient in the Italian central Alps suggests competition and facilitation among coniferous species. *Journal of Vegetation Science* 19:425–436, 2008.
- 570 Malandra, F., Vitali, A., Urbinati, C., Weisberg, P.J., Garbarino, M. Patterns and drivers of forest landscape change in the Apennines range, Italy. *Regional Environmental Change* 19:1973–1985. <https://link.springer.com/article/10.1007/s10113-019-01531-6>, 2019.
- Malanson, G. P., Resler, L. M., Bader, M. Y., Holtmeier, F. K., Butler, D. R., Weiss, D. J., Daniels, L. D., and Fagre, D. B. . Mountain treelines: A roadmap for research orientation. *Arctic, Antarctic, and Alpine Research*, 43(2), 167–177. doi: 10.1657/1938-4246-43.2.167, 2011.
- 575 McCune, B.. Improved estimates of incident radiation and heat load using non-parametric regression against topographic variables. *Journal of Vegetation Science* 18:751-754, 2007.
- Morales-Molino, C., Leunda, M., Morellón, M., Gardoki, J., Ezquerro, F. J., Muñoz Sobrino, C., Rubiales, J. M., and Tinner, W..Millennial land use explains modern high-elevation vegetation in the submediterranean mountains of Southern Europe. *Journal of Biogeography*, 49, 1779–1792. <https://doi.org/10.1111/jbi.14472>, 2022.
- 580 Morley, P. J., Donoghue, D. N. M., Chen, J. C., and Jump, A. S. . Integrating remote sensing and demography for more efficient and effective assessment of changing mountain forest distribution. In *Ecological Informatics* (Vol. 43, pp. 106–115). Elsevier B.V. doi: 10.1016/j.ecoinf.2017.12.002, 2018.



- Morley, P. J., Donoghue, D. N. M., Chen, J. C., and Jump, A. S.. Quantifying structural diversity to better estimate change at mountain forest margins. *Remote Sensing of Environment*, 223, 291–306. doi: 10.1016/J.RSE.2019.01.027, 2019.
- 585 Morresi, D., Vitali, A., Urbinati, C., and Garbarino, M. . Forest spectral recovery and regeneration dynamics in stand-replacing wildfires of central Apennines derived from Landsat time series. *Remote Sensing*, 11(3). doi: 10.3390/rs11030308, 2019.
- Motta, R., Morales, M., and Nola, P. Human land-use, forest dynamics and tree growth at the treeline in the Western Italian Alps. *Ann. For. Sci.* 63, 739–747. doi:10.1051/forest:2006055, 2006.
- Neeti, N., and Eastman, J. R.. A Contextual Mann-Kendall Approach for the Assessment of Trend Significance in Image Time Series. *Transactions in GIS*, 15(5), 599–611. doi: 10.1111/j.1467-9671.2011.01280.x, 2011.
- 590 Nguyen, T. A., Rußwurm, M., Lenczner, G., and Tuia, D. (2024). Multi-temporal forest monitoring in the Swiss Alps with knowledge-guided deep learning. *Remote Sensing of Environment*, 305. doi: 10.1016/j.rse.2024.114109
- Obojes, N., Buscarini, S., Meurer, A. K., Tasser, E., Oberhuber, W., Mayr, S., and Tappeiner, U. . Tree growth at the limits: the response of multiple conifers to opposing climatic constraints along an elevational gradient in the Alps. *Frontiers in Forests and Global Change*, 7. doi: 10.3389/ffgc.2024.1332941, 2024.
- 595 Pecher, C., Tasser, E., and Tappeiner, U.. Definition of the potential treeline in the European Alps and its benefit for sustainability monitoring. *Ecological Indicators*, 11(2), 438–447. <https://doi.org/10.1016/j.ecolind.2010.06.015>, 2011.
- Pesaresi, S., Biondi, E., and Casavecchia, S.. Bioclimates of Italy. *Journal of Maps*, 13(2), 955–960. <https://doi.org/10.1080/17445647.2017.1413017>, 2017.
- Piermattei, A., Garbarino, M., and Urbinati, C.. Structural attributes, tree-ring growth and climate sensitivity of *Pinus nigra* Arn. at high altitude: common patterns of a possible treeline shift in the central Apennines (Italy). *Dendrochronologia*, 32(3), 210–219. doi: 10.1016/J.DENDRO.2014.05.002, 2014.
- 600 Piper, F. I., Viñegla, B., Linares, J. C., Camarero, J. J., Cavieres, L. A., and Fajardo, A.. Mediterranean and temperate treelines are controlled by different environmental drivers. *Journal of Ecology*, 104(3), 691–702. doi: 10.1111/1365-2745.12555, 2016.
- 605 Potapov, P., Li, X., Hernandez-Serna, A., Tyukavina, A., Hansen, M. C., Kommareddy, A., Pickens, A., Turubanova, S., Tang, H., Silva, C. E., Armston, J., Dubayah, R., Blair, J. B., and Hofton, M.. Mapping global forest canopy height through integration of GEDI and Landsat data. *Remote Sensing of Environment*, 253. <https://doi.org/10.1016/j.rse.2020.112165>, 2021.
- Powell, S. L., Cohen, W. B., Healey, S. P., Kennedy, R. E., Moisen, G. G., Pierce, K. B., and Ohmann, J. L.. Quantification of live aboveground forest biomass dynamics with Landsat time-series and field inventory data: A comparison of empirical modeling approaches. *Remote Sensing of Environment*, 114(5), 1053–1068. <https://doi.org/10.1016/j.rse.2009.12.018>
- 610 Rivas-Martínez, S. (1993). Bases para una nueva clasificación. *Folia Botanica Madritensis*, 10, 1–23., 2010.
- Rumpf, S. B., Gravey, M., Brönnimann, O., Luoto, M., Cianfrani, C., Mariethoz, G., and Guisan, A.. From white to green: Snow cover loss and increased vegetation productivity in the European Alps. *Science*, 376, 1119–1122. doi: 0.1126/science.abn6697, 2022.
- 615 Schroeder, T. A., Wulder, M. A., Healey, S. P., and Moisen, G. G.. Mapping wildfire and clearcut harvest disturbances in boreal forests with Landsat time series data. *Remote Sensing of Environment*, 115(6), 1421–1433. <https://doi.org/10.1016/J.RSE.2011.01.022>, 2011.
- 620 Schultz, M., Clevers, J. G. P. W., Carter, S., Verbesselt, J., Avitabile, V., Quang, H. V., and Herold, M. . Performance of vegetation indices from Landsat time series in deforestation monitoring. *International Journal of Applied Earth Observation and Geoinformation*, 52, 318–327. <https://doi.org/10.1016/j.jag.2016.06.020>, 2016.
- Snethlage, M.A., Geschke, J., Spehn, E.M., Ranipeta, A., Yoccoz, N.G., Körner, Ch., Jetz, W., Fischer, M. and Urbach, D. A hierarchical inventory of the world's mountains for global comparative mountain science. *Nature Scientific Data*. <https://doi.org/10.1038/s41597-022-01256-y>, 2022a.
- 625 Snethlage, M.A., Geschke, J., Spehn, E.M., Ranipeta, A., Yoccoz, N.G., Körner, Ch., Jetz, W., Fischer, M. and Urbach, D. GMBA Mountain Inventory v2. *GMBA-EarthEnv*. <https://doi.org/10.48601/earthenv-t9k2-1407>, 2022b.
- Tarquini, S., Isola, I., Favalli, M., Battistini, A., and Dotta, G. . TINITALY, a digital elevation model of Italy with a 10 meters cell size (Version 1.1). Istituto Nazionale di Geofisica e Vulcanologia (INGV), <https://doi.org/10.13127/tinitaly/1.1>, 2023.
- 630



- Tian, L., Fu, W., Tao, Y., Li, M., and Wang, L.. Dynamics of the alpine timberline and its response to climate change in the Hengduan mountains over the period 1985–2015. *Ecological Indicators*, 135. <https://doi.org/10.1016/j.ecolind.2022.108589>, 2022.
- 635 Tolan, J., Yang, H. I., Nosarzewski, B., Couairon, G., Vo, H. v., Brandt, J., Spore, J., Majumdar, S., Haziza, D., Vamaraju, J., Moutakanni, T., Bojanowski, P., Johns, T., White, B., Tiecke, T., and Couprie, C.. Very high resolution canopy height maps from RGB imagery using self-supervised vision transformer and convolutional decoder trained on aerial lidar. *Remote Sensing of Environment*, 300. <https://doi.org/10.1016/j.rse.2023.113888>, 2024.
- Tucker, C. J.. Red and Photographic Infrared Linear Combinations for Monitoring Vegetation. *Remote Sensing of Environment*, 8, 127–150. Retrieved from [http://dx.doi.org/10.1016/0034-4257\(79\)90013-0](http://dx.doi.org/10.1016/0034-4257(79)90013-0), 1979.
- 640 Vacchiano, G., Garbarino, M., Lingua, E., and Motta, R.. Forest dynamics and disturbance regimes in the Italian Apennines. *Forest Ecology and Management*, 388, 57–66. <https://doi.org/10.1016/j.foreco.2016.10.033>, 2017.
- Vitali, A., Camarero, J. J., Garbarino, M., Piermattei, A., and Urbinati, C.. Deconstructing human-shaped treelines: Microsite topography and distance to seed source control *Pinus nigra* colonization of treeless areas in the Italian Apennines. *Forest Ecology and Management*, 406, 37–45. doi: 10.1016/j.foreco.2017.10.004, 2017.
- 645 Vitali, A., Urbinati, C., Weisberg, P. J., Urza, A. K., and Garbarino, M.. Effects of natural and anthropogenic drivers on land-cover change and treeline dynamics in the Apennines (Italy). *Journal of Vegetation Science*, 29(2), 189–199. doi: 10.1111/jvs.12598, 2018.
- Wang, X. L., and Swail, V. R.. Changes of extreme Wave Heights in northern Hemisphere Oceans and related atmospheric circulation regimes. *Journal of Climate*, 14(10), 2204–2221. doi: 10.1175/1520-0442(2001)014<2204:COEWHI>2.0.CO;2, 2001.
- 650 Wei, C., Karger, D. N., and Wilson, A. M. . Spatial detection of alpine treeline ecotones in the Western United States. *Remote Sensing of Environment*, 240. <https://doi.org/10.1016/j.rse.2020.111672>, 2020.
- Wilcoxon F. Individual comparisons by ranking methods. *Biometrics* 1:80–83, 1945.
- Wood, S.N. Fast stable restricted maximum likelihood and marginal likelihood estimation of semiparametric generalized linear models. *Journal of the Royal Statistical Society (B)* 73(1):3–36, 2011.
- 655 Zhou, M., Li, D., Liao, K., and Lu, D. . Integration of Landsat time-series vegetation indices improves consistency of change detection. *International Journal of Digital Earth*, 16(1), 1276–1299. doi: 10.1080/17538947.2023.2200040, 2023.
- Zhu, Z.. Change detection using landsat time series: A review of frequencies, preprocessing, algorithms, and applications. *ISPRS Journal of Photogrammetry and Remote Sensing*, 130, 370–384. doi: 10.1016/J.ISPRSJPRS.2017.06.013, 2017.
- 660 Zou, F., Tu, C., Liu, D., Yang, C., Wang, W., and Zhang, Z. . Alpine Treeline Dynamics and the Special Exposure Effect in the Hengduan Mountains. *Frontiers in Plant Science*, 13. <https://doi.org/10.3389/fpls.2022.861231>, 2022.